JOURNAL OF APPLIED CRYSTALLOGRAPHY

Volume 49 (2016)

Supporting information for article:

Martensite Adaption through Epitaxial Nano Transition Layers in TiNiCu Shape Memory Alloys

Torben Dankwort, Julian Strobel, Christoph Chluba, Wenwei Ge, Viola Duppel, Manfred Wuttig, Eckhard Quandt and Lorenz Kienle

Supporting information

Table S1 Elemental composition as determined by EDX point measurements. (Mean atomic composition m_X and standard deviation σ_X have been calculated from 111 different measurements for B2/B19, 20 measurements for Ti_2Cu and 7 measurements for Ti_2Ni)

	m_{Ti} [at%]	σ_{Ti} [at%]	m_{Ni} [at%]	σ_{Ni} [at%]	m_{Cu} [at%]	σ_{Cu} [at%]
B2/B19	52.4	±2.7	34.2	±2.1	13.4	±1.8
Ti_2Cu	62.6	±3.4	23.6	±4.8	13.8	±3.4
Ti_2Ni	65.1	±6.1	28.9	±4.5	6.0	±2.1

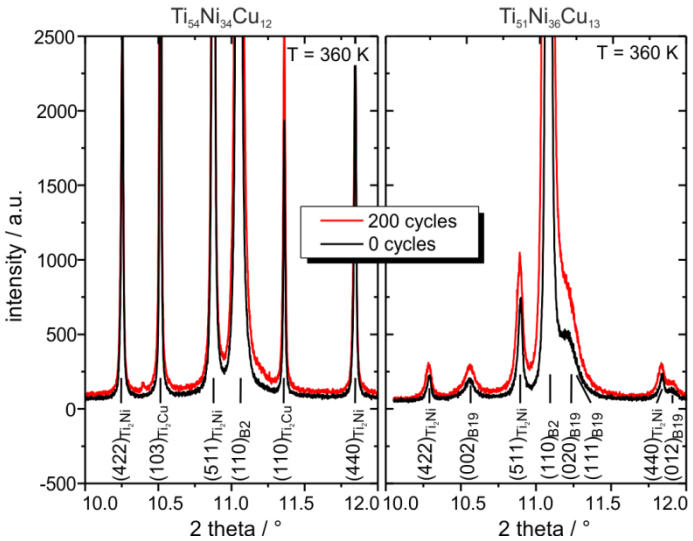

Figure S1 Synchrotron XRD investigations for different compositions and cycling states. Measurement temperature is 360 K, which is above A_f for both alloys. Only the Ti-rich composition (left) contains the presumably critical precipitate of the Ti_2Cu-type. The Ti-poor compound (right) contains residual B19, whose fraction increases upon cycling as evident from the increasing peak intensity. This finding has been confirmed by Rietveld refinement. For a more detailed listing of constituent phases consult Chluba et al., 2015.

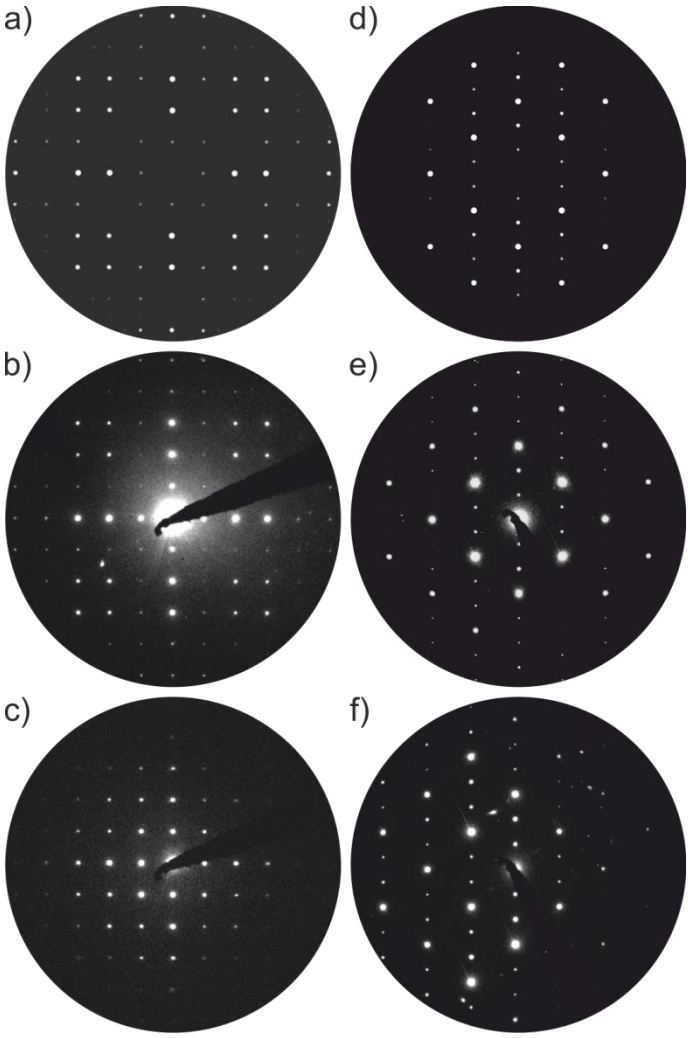

Figure S2 Experimental diffraction patterns (PED b) and e); SAED c) and f)) next to simulated diffraction patterns (a) and d)) of Ti_2Ni (left column) and Ti_2Cu (right column). Both zone axes (ZA) are [100].

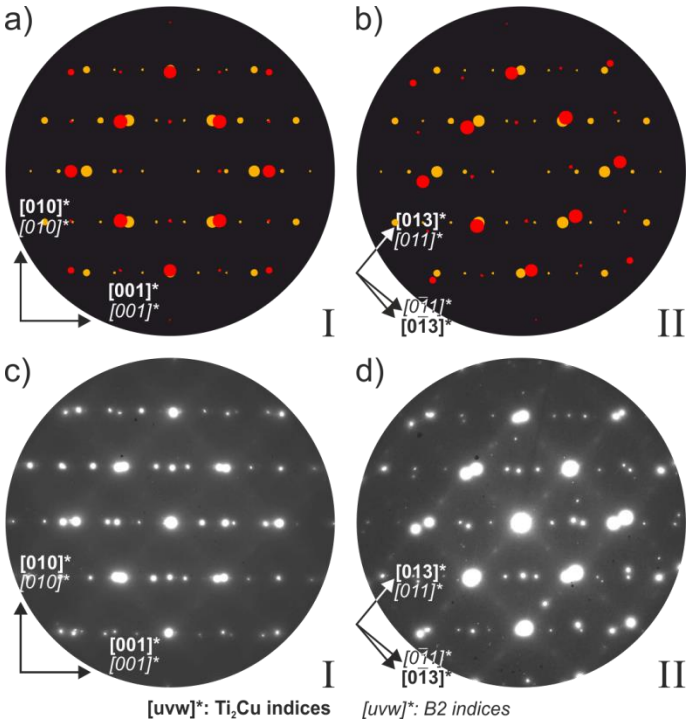

Figure S3 Simulated superposition diffraction patterns of B2 (red) and Ti_2Cu (yellow). ZAs are [100] for both phases. a) variant I, b) variant II. The corresponding parallel strain is a) 2.80 % and b) -6.15 %. For calculation of the strain values see Chluba et al, 2015. c) and d) are the corresponding experimentally found diffraction patterns.

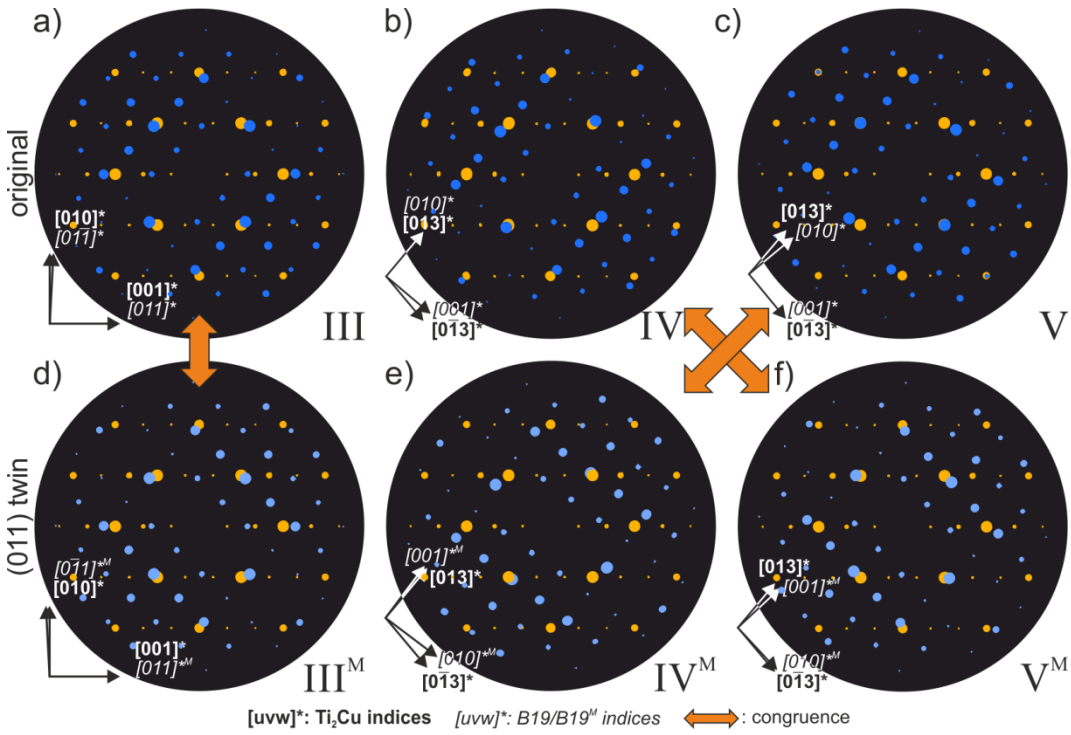

Figure S4 Superposition of simulated diffraction patterns of B19 (blue), $B19^M$ (light blue) and Ti_2Cu (yellow). ZAs are [100] for all phases. a) variant III, b) variant IV, c) variant V. d) to f) represent the interfaces of a) to c) with the B19 (011) compound twin instead of the non-mirrored variant, variants III^M to V^M. Orange arrows indicate (almost) congruence of indicated patterns. Parallel strain for the different interfaces: a) and d): 5.18%; b): -7.02%; c): -1.28 %. For calculation of the strain values see Chluba et al., 2015. The strain is easily visible from the splitting of reflections orthogonally to the habit planes, e.g. the splitting of the 010_{Ti_2Cu} and $01\text{-}1_{B19}$ reflections in a).

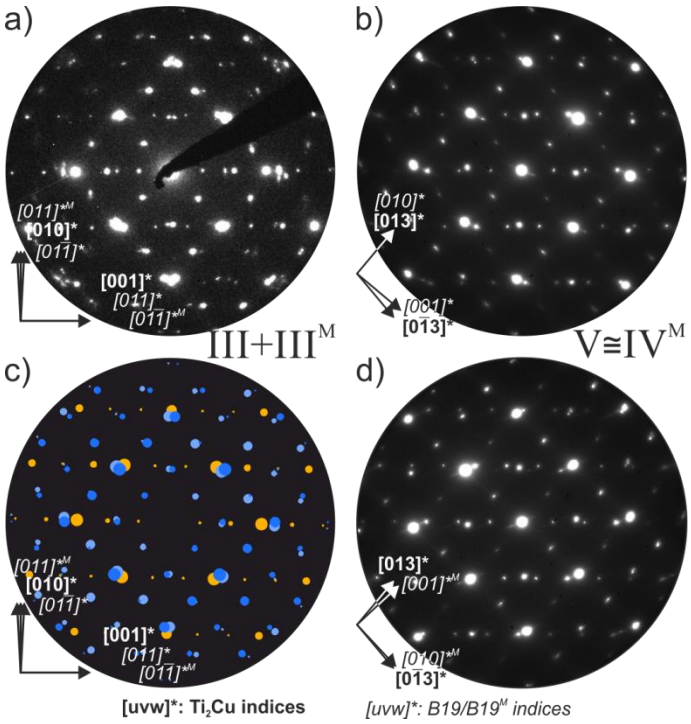

Figure S5 Experimentally observed diffraction patterns as predicted for the B19/Ti_2Cu interface. ZAs are [100] for both phases. The diffraction pattern in a) contains both the variants III and III^M; c) is the addition of both of these simulations. The DPs b) and d) are mirror images of each other. As described above the patterns for both situations are indistinguishable, they correspond to variants V and IV^M.

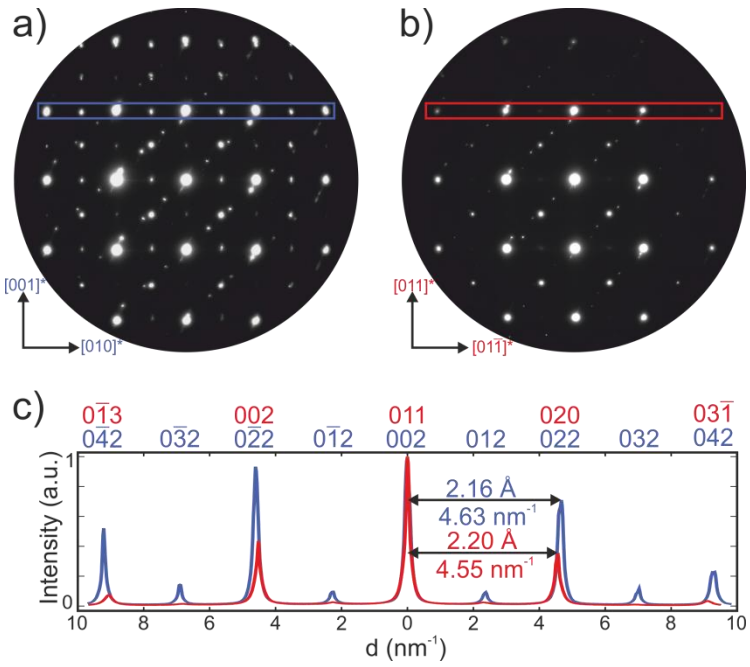

Figure S6 Vanishing of B19 Reflections (012 etc) and shrinking of reciprocal distance as expected for a B19-B2 transition. a) SAED at -15 °C immediately after finding the sample area, b) after several minutes of exposure to the electron beam c) line profiles of marked areas in a) and b) from the color coded areas. Profiles underline the vanishing of B19 specific reflections (012, 0-12 etc) and shrinking of reciprocal distances as expected.